时效对 Sn-Zn 无铅钎料焊点可靠性的影响

胡玉华[1]， 薛松柏[1]， 杨晶秋[2] 叶 焕[1]， 顾立勇[3]， 顾文华[3]
(1. 南京航空航天大学 材料科学与技术学院，南京 210016；2. 哈尔滨焊接研究所，哈尔滨 150080；
3. 常熟市华银焊料有限公司，常熟 215513)


胡玉华

摘 要：采用扫描电子显微镜及 STR-1000 微焊点强度仪器，研究了 Sn-9Zn-0.06Nd/Cu 钎焊接头在 150 ℃时效过程中界面组织形貌和力学性能的变化. 结果表明，Sn-9Zn-0.06Nd/Cu 接头焊接后的界面生成了较为平坦的金属间化合物层 Cu_5Zn_8，随着时效时间的增加，金属间化合物层不断增厚. 经过时效处理，钎料中的稀土元素 Nd 向界面富集并在界面附近生成了 Nd_3Sn 相，同时微焊点的拉伸力不断减小，当时效 720 h 后，焊点的拉伸力下降了近 50%. 时效后焊点断裂方式由韧性断裂向脆性断裂转变.

关键词：时效；金属间化合物；界面组织；力学性能
中图分类号：TG454 **文献标识码**：A **文章编号**：0253-360X(2012)03-0041-04

0 序 言

传统电子行业中，SnPb 钎料凭借着较低熔点和优良的润湿性能而被广泛应用. 铅及其化合物是有毒物质，随着对环境保护的重视，许多国家已通过一系列的法律限制含铅产品的使用[1,2]，促进了无铅钎料的开发和研究. 其中 Sn-Zn 系钎料被认为是具有广阔应用前景的无铅钎料之一.

产品的服役过程中钎料作为实现组件与 PCB 基板之间电气和机械的连接材料，环境温度以及电路的周期性通断会在其焊点内部产生周期性应力应变，诱发裂纹的萌生和扩展，致使焊点失效，因此对钎料焊点的可靠性研究是至关重要的[3]. 稀土元素被称为是金属材料中的“维他命”，即金属材料中稀土元素的加入能够改善和优化材料的性能. 国内外研究者们通过采用混合添加和单一添加的不同方式向无铅钎料中添加稀土元素，研究了稀土元素的添加对钎料本身性能的影响[4-6]. 其中对稀土元素 Nd 的添加鲜见报道，在前期的工作中课题组研究了 Nd 元素的添加量对 Sn-9Zn 合金钎料润湿性能、力学性能等的影响，发现当稀土元素 Nd 的添加量为 0.06%(质量分数)时钎料的综合性能最佳[7]. 因此试验主要以 Sn-9Zn-0.06Nd 为对象，研究了 Sn-9Zn-0.06Nd/Cu 钎焊接头在长时间时效过程中界面组织形貌及接头力学性能的变化，为 Sn-Zn 系钎料的可靠性研究提供理论指导.

1 试验方法

1.1 合金熔炼

试验所用 Sn-9Zn-0.06Nd 钎料由纯度为 99.99% 的金属锡、锌和粉末钕用电子天平(精度 0.01 g)按比例逐一称取，在温度为 500 ℃的坩埚电阻炉中，氮气和熔盐(LiCl: KCl = 1: 1.3)的保护作用下熔炼 3 h 而成. 熔炼期间每隔 20 min 进行搅拌，促进合金的均匀化.

1.2 时效处理

1.2.1 界面试样制备

Sn-9Zn-0.06Nd/Cu 界面焊接示意图如图 1 所示. 铜基板为紫铜板(40 mm × 40 mm × 2 mm)，钎料为 0.2 g，钎剂为 $ZnCl_2$-NH_4Cl 溶液. 焊接前将铜

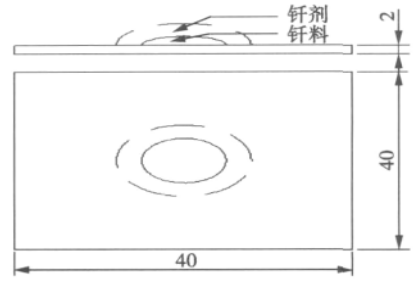

图 1 Sn-9Zn-0.06Nd/Cu 界面焊接示意图(mm)
Fig. 1 Soldering diagram for Sn-9Zn-0.06Nd/Cu interface

收稿日期：2011-12-09
基金项目：2010 年度江苏省企业研究生工作站资助项目

基板用砂纸打磨光滑并用酒精进行清洗，放置于温度为 250 ℃的箱式电阻炉中，保温 3 min 后拿出，冷却后用酒精将表面清洗干净.

1.2.2 拉伸试样制备

为模拟实际生产，采用 PCB 基板为锡镀层的焊盘、QFP 器件进行焊接. 将上述试样放置于设置温度为 150 ℃的烘箱中，进行 72，168，240，360，720 h 不同时间段的时效处理，来观测钎焊接头的界面组织形貌以及力学性能的变化.

1.2.3 组织观察和拉伸性能测试

从中间截取用环氧树脂镶样后，经过粗磨、细磨、抛光、腐蚀(4% HNO_3 酒精溶液) ，采用扫描电镜对不同时效时间的 Sn-9Zn-0.06Nd/Cu 界面组织进行观察和分析.

焊点的拉伸力采用日本 Rhesca 公司的 STR-1000 微焊点强度测试仪进行检测，试验装置如图 2 所示. 试验依据日本工业标准 JIS Z 3198—6—2003《无铅钎料试验方法—第 6 部分: QFP 引脚焊点的 45°角拉脱试验方法》的有关规定[8] 进行.

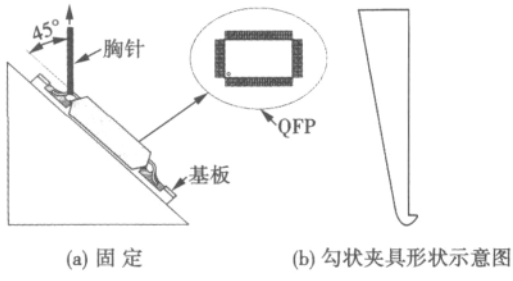

图 2 引脚拉伸力测试方法

Fig. 2 Test method for pull force

2 试验结果与分析

图 3 为 Sn-9Zn-0.06Nd/Cu 钎焊接头在 150 ℃下不同时效时间的界面组织形貌. 钎焊后钎料与铜基板界面生成了一层平坦的金属间化合物层如图 3a 所示，由 EDX 成分分析可知该金属间化合物为 Cu_5Zn_8. 在 150 ℃温度下对钎焊接头进行了时效处理，钎料中的 Zn 元素向界面处扩散，金属间化合物层厚度增加，如图 3b 所示，当时效 72 h 后界面附近出现了白色金属间化合物相，经 EDX 成分分析该化合物相为 Nd_3Sn. 稀土元素作为表面活性元素，容易向晶界及表面处聚集[9]. 随着时效时间的增长，钎料中的稀土元素 Nd 不断向界面处富集，从而导致了界面附近 Nd_3Sn 化合物相的增多. 当时效时间达到 720 h 之后，钎料中也出现了少量的 Cu_5Zn_8 相. 这是由于在 150 ℃的温度下基板中的 Cu 元素亦不断向钎料中扩散，从而导致了钎料中少量 Cu_5Zn_8 相的生成.

图 4 为利用 Image-ProPlus 6.0 软件测出的界面 IMC 厚度随时效时间的变化情况. 由图 4 可以看出，Sn-9Zn-0.06Nd/Cu 界面 IMC 厚度随着时效时间的平方根成正比，满足菲克扩散方程，即

$$d - d_0 = (kt)^{1/2}$$

式中: d 为界面层厚度; d_0 为界面层初始厚度; k 为

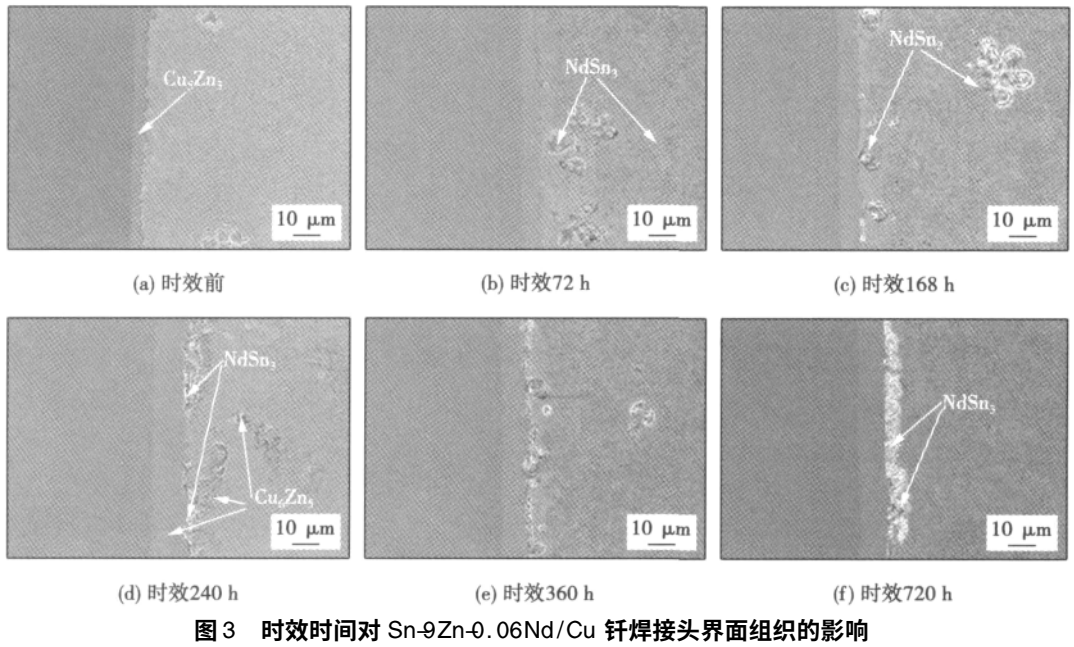

图 3 时效时间对 Sn-9Zn-0.06Nd/Cu 钎焊接头界面组织的影响

Fig. 3 Cross-sectional images of Sn-9Zn-0.06Nd/Cu interfaces with different age time

生长速率常数；t 为时效时间.

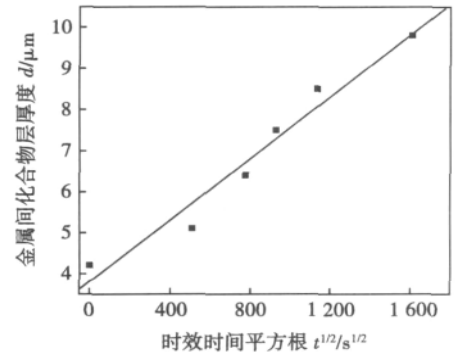

图 4　时效时间对 Sn-9Zn-0.06Nd/Cu 界面 IMCs 厚度的影响

Fig. 4　Average thickness of IMLs of Sn-9Zn-0.06Nd/Cu joints with different aging time

图 5 为 Sn-9Zn-0.06Nd/Cu 微焊点拉伸力随着时效时间增加的变化情况. 随着时效时间的增加，焊点的拉伸力不断下降. 当时效时间达到 720 h 后，焊点的拉伸力下降了近 50%. 由此可见，时效过程对焊点的力学性能影响较大，这主要是因为随着时效时间的增加，界面处大量 Nd_3Sn 化合物的生成，这些金属间化合物是脆性相，在外加载荷的作用下容易形成应力集中区，从而导致裂纹的萌生、扩展，引起失效.

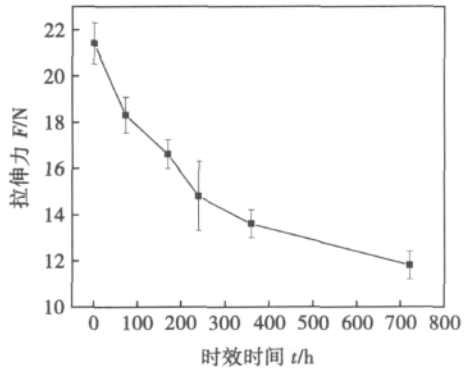

图 5　时效时间对 Sn-9Zn-0.06Nd/Cu 微焊点拉伸力的影响

Fig. 5　Pull force of Sn-9Zn-0.06Nd/Cu with different aging time

图 6 为不同的时效时间下 Sn-9Zn-0.06Nd/Cu 钎焊接头的断口形貌，接头的断裂位置随着时效时间的增加而发生变化. 图 6a 为时效前的试样在外加载荷作用下发生断裂的断口形貌，断口处有大量的韧窝，在钎料的内部发生韧性断裂[10,11]. 当时效时间达 168 h 之后，断口形貌如图 6b 所示，韧窝变大，在韧窝底部出现了细小颗粒，经分析发现该颗粒为 Cu_5Zn_8 化合物. 时效 720 h 之后如图 6c 所示，韧窝面积减少，局部出现了脆性断裂的特征，这说明断裂发生于界面化合物层和少量钎料边缘，焊接接头的断裂方式由韧性断裂转变为局部脆性断裂. 时效 720 h 之后，界面金属间化合物层的不断增厚，同时生成的大量 Nd_3Sn 相，降低了接头的连接强度.

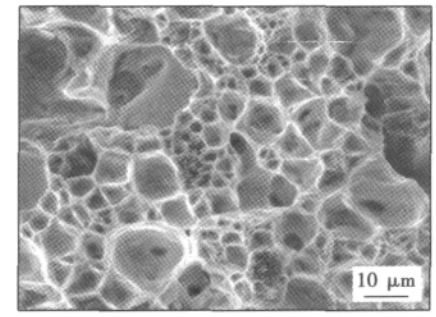

(a) 时效前

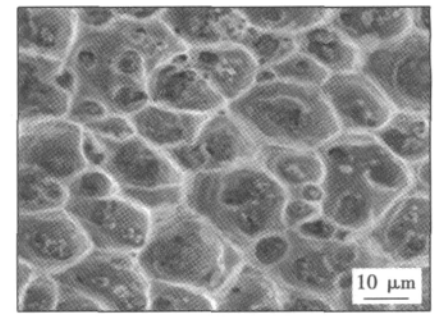

(b) 时效168 h

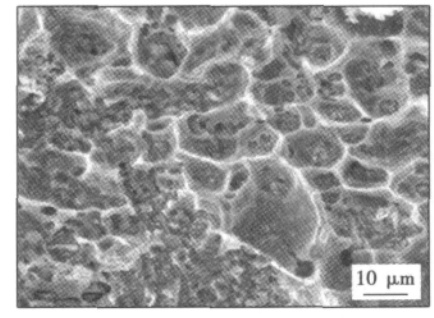

(c) 时效720 h

图 6　不同时效时间下的 Sn-9Zn-0.06Nd/Cu 接头断口形貌

Fig. 6　Fracture morphologies of Sn-9Zn-0.06Nd/Cu soldered joints aged for different time

3　结　论

(1) Sn-9Zn-0.06Nd/Cu 接头焊接后的界面生成了较为平坦的金属间化合物层 Cu_5Zn_8，随着时效时间的增加，金属间化合物层不断增厚. 经过时效处理，钎料中的稀土元素 Nd 向界面富集并在界面附近生成了 Nd_3Sn 相.

(2) 随着时效处理的进行,Sn-9Zn-0.06Nd/Cu 微焊点的拉伸力不断减小,当时效 720 h 后,与时效前相比焊点的拉伸力下降了近 50%. 随着时效的进行,焊点的断裂位置由时效前的焊点内部转移到界面化合物处,断裂方式由时效前的韧性断裂转变成局部脆性断裂.

参考文献:

[1] 杨 磊,郭 黎,揭晓华. 新型无铅焊料 Sn-X-Cu-Ni 的性能研究[J]. 热加工工艺,2010,39(3):138-140.
Yang Lei, Guo Li, Jie Xiaohua. Property of new type lead-free solder Sn-X-Cu-Ni [J]. Hot Working Technology, 2010, 39(3):138-140.

[2] Suganuma K. Advances in lead-free electronics soldering [J]. Current Opinion in Solid State and Materials Science, 2001, 5(1): 55-64.

[3] Zeng K, Tu K N. Six cases of reliability study of Pb-free solder joints in electronic packaging technology [J]. Materials Science and Engineering, 2002, 38(1): 55-105.

[4] Chen W, Kong J. Effect of rare earth Ce on the microstructure, physical properties and thermal stability of a new lead-free solder [J]. Journal of Mining and Metallurgy Section B-Metallurgy, 2011, 47(1): 11-21.

[5] Zhang L, Xue S B, Gao L L. Development of Sn-Zn lead-free solders bearing alloying elements [J]. Journal of Materials Science-Materials in Electronics, 2010, 21(1): 1-15.

[6] 陈志刚,史耀武,夏志东,微量混合稀土对 SnAgCu 钎料合金性能的影响[J]. 电子工艺技术,2003,24(2): 53-58.
Chen Zhigang, Shi Yaowu, Xia Zhidong. Effect of mixed rare earth on the properties of snagcu lead-free solder alloy [J]. Electronics Process Technology, 2003, 24(2): 53-58.

[7] Hu Y H, Xue S B, Wang H. Effects of rare earth element Nd on the solderability and microstructure of Sn-Zn lead-free solder [J]. Journal of Materials Science-Materials in Electronics, 2011, 22(5): 481-487.

[8] 王春青,李明雨,田艳红,等. JIS Z 3198 无铅钎料试验方法简介与评述[J]. 电子工艺技术,2004,25(2): 47-53.
Wang Chunqing, Li Mingyu, Tian Yanhong, *et al*. Review of JIS Z 3198 test method for lead-free solders [J]. Electronics Process Technology, 2004, 25(2): 47-53.

[9] Chen Z G, Shi Y W, Xia Z D. Study on the microstructure of a novel lead-free solder alloy SnAgCu-RE and its soldered joints [J]. Journal of Electronic Materials, 2002, 31(10), 1122-1128.

[10] Han Z J, Xue S B, Wang J X. Mechanical properties of QFP micro-joints soldered with lead-free solders using diode laser soldering technology [J]. Transactions of Nonferrous Metals Society of China, 2008, 18(4): 814-818.

[11] Chen W X, Xue S B, Wang H, *et al*. Investigation on properties of Ga to Sn-9Zn lead-free solder [J]. Journal of Materials Science: Materials in Electronics, 2010, 21(5): 496-502.

作者简介: 胡玉华,女,1987 年出生,硕士研究生. 主要从事微电子焊接技术及无铅钎料的研究工作. 发表论文 4 篇. Email: huyuhua_2006@126.com

通讯作者: 薛松柏,男,教授. Email: xuesb@nuaa.edu.cn

书 讯

书号:978-7-111-33462-0
定价:158.00元

《三元合金相图手册》

张启运 庄鸿寿 编

◇选录了文献中发表过的近千幅三元合金相图,便于读者查阅。
◇概略叙述了必要的相图基础,对初涉相图的读者有所帮助。
◇列出了金属元素的物理、化学和力学性质、便于读者分析相图。

本书列出了金属元素的物理、化学和力学性质,这些数据对相图的实践分析有很重要的意义。在这里将元素有关数据以填入周期表的方式表达出来,不但查阅方便,更有利于观察元素性质之间的相互辩证关联;还搜集了至 2011 年初为止的近千幅常用三元合金相图,便于读者查阅。

本书采用简单、易懂的语言概略叙述了必要的相图基础,可供工程技术、材料科学、物理、化学等有关领域的学者和技术人员和高等学校有关学科的师生参考。

编辑热线:010-88379733 购书热线:010-88379405 传真:010-68351729 网络购书支持:中国科技金书网

传真购书请注明:姓名、详细地址、邮编、联系电话、传真、E-mail、所购图书书名、书号、数量、是否需要发票及发票抬头

sion, which makes it possible to weld large and thick plates without back chipping. The pulsed TIG welding is an optimal choice for backing welding of large and thick plates. Both sides of the groove root melt during the peak current period due to the strong melting ability of the arc. The welding pool rapidly solidifies during the base current period, preventing the dropping of welding pool. During misplacing and synchronizing double-sided backing welding, the rear arc leads to an increment of the high temperature area in the workpiece and elongation of the front pool. The macrograph of the weld shows that the base metal sufficiently melts and the lateral wall fuses well. The weld surface is smooth with no pores, cracks and inclusions.

Key words: double-sided arc; backing weld; large thick plate; characteristics of pool formation; root fusion

Effects of aging treatment on reliability of SnZn soldered joints HU Yuhua[1], XUE Songbai[1], Yang Jingqiu[2], YE Huan[1], GU Liyong[3], GU Wenhua[3] (1. School of Materials Science and Technology, Nanjing University of Aeronautics and Astronautics, Nanjing 210016, China; 2. Harbin Welding Institute, Harbin 150080, China; 3. Changshu Huayin Filler Metals Co., Ltd., Changshu 215513, China). pp 41 – 44

Abstract: The interface morphology and mechanical property of Sn-9Zn-0.06Nd/Cu soldered joints after aging treatment at 150 ℃ were investigated with scanning electronic microscope (SEM) and STR-1000 joint strength tester. The experimental results indicated that a planar Cu_5Zn_8 intermetallic layer (IMC) formed in the soldered joint interface, whose thickness increased with increasing aging time, and the rare earth element Nd migrated towards the interface and reacted with Sn forming Nd_3Sn near the interface. While increasing the aging time, the tensile stress of the Sn-9Zn-0.06Nd/Cu micro-joints decreased, and it even reduced by 50% after aging for 720 h. The fracture mode of the soldered joints turned from ductile fracture before aging treatment to both ductile and brittle fracture after aging for 720 h.

Key words: aging treatment; intermetallic compound; interface morphology; mechanical property

Welding deformation prediction and structure optimization of air conditioning compressor based on FEM LI Yongzhi[1], LU Hao[1], CHEN Junmei[1], REN Liping[2] (1. School of Materials Science and Engineering, Shanghai Jiao Tong University, Shanghai 200240, China; 2. Engineering Research Center, Gree Electric Appliances, Inc., Zhuhai 519070, China). pp 45 – 48

Abstract: A thermal elastic-plastic finite element model is established to simulate the three-point welding of compressor shell and cylinder. Several sensitivity parameters are discussed such as the height of the compressor shell, the material properties of the cylinder and the wall thickness in specific locations of the cylinder. The width change becomes smaller when the cast steel is used for the cylinder material, and the contact condition between the cylinder and the shell has significant effects on the deformation of the cylinder. In order to improve the efficiency of calculating and maintain the accuracy of the results, an inherent strain FE model based on the thermal elastic-plastic finite element model is developed. The result obtained by using the inherent strain method agrees well with both the thermal elastic-plastic result and the experimental result. Moreover, the inherent strain method can greatly reduce the computing time. This method can be applied in optimization of large and complex welded structures.

Key words: thermal elastic-plastic FEM; inherent strain method; air conditioning compressor; welding deformation

Analysis on WC-8Co electro-spark deposition coating with powder presetting method GAO Yuxin[1,2], ZHAO Cheng[1], YI Jian[2,3] (1. Surface Engineering Laboratory, Qingdao University of Science and Technology, Qingdao 266061, China; 2. College of Mechanical Engineering, Taizhou University, Taizhou 318000, China; 3. State Key Laboratory of New Ceramics and Fine Processing, Tsinghua University, Beijing 100084, China). pp 49 – 52

Abstract: To improve the deficiencies in traditional electro-spark deposition (ESD) process, such as complicated preparation of electrodes and existence of cracks or holes in the coatings, a new ESD coating process was proposed by presetting WC-8Co powder in the plasma channal between the electrode and substrate. The surface morphology, microstructure and abrasion properties of the coating made with the new process were investigated and compared with the traditional ESD process. The results showed that the new process could produce a dense coating with low surface roughness which metallurgically bonded with the substrate. The coating prepared with the new process had better abrasion resistance than that with the traditional process. Preparation of ESD coating with powder presetting method could improve the efficiency of electro-spark deposition technique, and was suitable for producing coatings with large area.

Key words: electro-spark deposition; powder presetting; powder process; abrasion resistance

In-situ observation of residual liquid metal during laser welding of austenite stainless steels WEN Peng[1,2], SHINOZAKI Kenji[3], YAMAMOTO Motomichi[3] (1. Mechanical Engineering Department, Tsinghua University, Beijing 100084, China; 2. Key Laboratory of Advanced Materials, Ministry of Education, Tsinghua University, Beijing 100084, China; 3. Mechanical Engineering Department, Hiroshima University, Hiroshima 739-8527, Japan). pp 53 – 56

Abstract: The high cooling rate during laser welding process may prompt the occurrence of solidification cracking, which is directly related to the existence of residual liquid metal in the solidification temperature range. In this paper, the in-situ observation of residual liquid metal at the trailing edge of the weld pool with optical microscope was conducted directly with high speed and high magnification during laser welding of SUS304, SUS316 and SUS310S austenite stainless steels. The solidification behavior under different welding speeds was analyzed. It was found that the in-situ observed residual liquid metal was a part of the coexistence zone of liquid and solid during solidification process. The order of in-situ observed existence range of residual liquid metal was in good correspondence with the solidification cracking susceptibility, which was obtained by fan-shaped hot cracking test.

Key words: laser welding; solidification cracking; residual liquid metal; in-situ observation